Current Applied Physics 11 (2011) S296–S300

Contents lists available at ScienceDirect

Current Applied Physics

journal homepage: www.elsevier.com/locate/cap

Vacancy defects in indium oxide: An *ab-initio* study

Pakpoom Reunchan [a,b], Xin Zhou [a,c], Sukit Limpijumnong [b,d,*], Anderson Janotti [e], Chris G. Van de Walle [e]

[a] Asia Pacific Center for Theoretical Physics, Pohang, Gyeongbuk 790-784, Republic of Korea
[b] School of Physics, Suranaree University of Technology and Synchrotron Light Research Institute, Nakhon Ratchasima 30000, Thailand
[c] Department of Physics, Pohang University of Science and Technology, Pohang, Gyeongbuk 790-784, Republic of Korea
[d] Thailand Center of Excellence in Physics (ThEP Center), Commission on Higher Education, Bangkok 10400, Thailand
[e] Materials Department, University of California, Santa Barbara, California 93106, United States

ARTICLE INFO

Article history:
Received 28 September 2010
Received in revised form
8 March 2011
Accepted 14 March 2011
Available online 21 March 2011

Keywords:
First-principles calculations
Vacancy defects
Indium oxide

ABSTRACT

First-principles density functional theory is employed to study the electrical behavior of oxygen and indium vacancies in indium oxide (In_2O_3). The oxygen vacancy is found to be a double donor. The indium vacancy is a triple acceptor, which >can be a compensation center in *n*-type In_2O_3, leading to *n*-type carrier reduction. However, its high formation energy under *p*-type conditions makes it unlikely to be a source of *p*-type carriers by itself.

1. Introduction

Transparent conducting oxides (TCOs) have attracted a lot of interest because of their unique characteristic of having simultaneously high visible-light transparency and high electrical conductivity. They can be used as transparent electrodes in light-emitting diodes, solar cells, and flat-panel displays. They can also be used as transparent heat-mirror coatings because of their high infrared (IR) reflectivity [1–3]. Sn-doped In_2O_3, which is called indium tin oxide (ITO), is the most widely used TCOs that can support very high carrier concentrations (up to 10^{21} cm^{-3}) and still maintain high optical transparency (>80%) [1,2]. Recently, hydrogen-doped In_2O_3 was also found experimentally to exhibit high carrier concentration with high mobility [3]. Theoretical studies by our group [4] also found H to act as a shallow donor in In_2O_3, consistent with the experimental observation. Amorphous or polycrystalline In_2O_3, grown by large-area deposition techniques, such as chemical vapor deposition and spray pyrolysis, is popularly used as transparent electrodes due to their relatively low fabrication cost. With more effort, single-crystal In_2O_3 can also be fabricated. Aside from its function as a transparent electrode, In_2O_3 is very attractive as a semiconductor by itself. This is partly due to the possibility of growing high quality In_2O_3 thin films. However, the challenges are to control the unintentional *n*-type conductivity of In_2O_3 and to dope it *p*-type. Therefore, understanding the effects of electrically active defects is a crucial step to manipulating the electrical properties of In_2O_3.

It is well known that nominally undoped bulk crystals and thin films of In_2O_3 exhibit a high level of *n*-type conductivity (10^{18}–10^{20} carriers/cm^{-3}) [5–7]. However, the cause of unintentional *n*-type conductivity in In_2O_3 remains unclear. Like other oxides (such as ZnO and SnO_2), the unintentional *n*-type conductivity in In_2O_3 has been attributed to the presence of native defects such as O vacancies and In interstitials. This is purely because the conductivity in oxides is often observed to vary with the oxygen partial pressure in the growth or annealing environments [8–10]. Recently, first-principles calculations based on the LDA + *U* and GGA + *U* approaches [11,12] found that O vacancies cannot be responsible for conductivity in undoped ZnO and SnO_2 because they are deep donors. In addition, it was found that Zn and Sn interstitials in ZnO and SnO_2 have very high formation energies in *n*-type samples although they are shallow donors. These cation interstitials also have very low migration barriers, making them unstable, since they will easily diffuse out of the crystal. These recent computational results on ZnO and SnO_2 raise the question whether native point defects are responsible or not for the observed *n*-type conductivity in In_2O_3. Acceptor-type defects such as the cation vacancies are also important because they can act as compensating

* Corresponding author. School of Physics, Suranaree University of Technology and Synchrotron Light Research Institute, Nakhon Ratchasima 30000, Thailand. Tel.: +66 44 22 4619.
E-mail address: sukit@sut.ac.th (S. Limpijumnong).

1567-1739/$ – see front matter © 2011 Elsevier B.V. All rights reserved.
doi:10.1016/j.cap.2011.03.051

centers in *n*-type material. In the case of In_2O_3, In vacancies may act as compensation centers, reducing the electron concentration in transparent contacts.

In this paper, we report first-principles DFT calculations of electronic and structural properties of O and In vacancies (V_O and V_{In}) in In_2O_3. The error in the DFT–LDA band gap can cause large uncertainties in the calculated transition levels and formation energies. Therefore, corrections to the calculated transition levels and formation energies are crucial for the results to be directly compared with experiments. Here, we use a previously established approach based on DFT–LDA and LDA + *U* calculations [11], which has been successfully applied to the case of native point defects in ZnO [11].

2. Computational details

Our first-principles calculations are based on density functional theory (DFT) using the projector-augmented-wave (PAW) method as implemented in the VASP code [13–16]. We used the local density approximation (LDA) and the LDA + *U* for the exchange-correlation potential. The vacancy defect is created by removing an O atom (for V_O) or an In atom (for V_{In}) from a 80-atom bixbyite supercell [space group $T_h^7(Ia\bar{3})$] of In_2O_3. We used a shifted $2 \times 2 \times 2$ Monkhorst-Pack set of special *k* points (to avoid the Γ point) for the integration over the Brillouin zone. A plane-wave basis set with an energy cutoff of 400 eV is used. All the calculations were performed at the calculated equilibrium lattice constants where all the atoms are relaxed until the residual forces become less than 0.015 eV/Å.

The likelihood of forming a vacancy in In_2O_3 can be determined by calculating their formation energies. The formation energy of an oxygen vacancy in charge state *q* is defined as

$$E^f(V_O^q) = E_{tot}(V_O^q) - E_{tot}(In_2O_3) + \mu_O + qE_F, \quad (1)$$

where $E_{tot}(V_O^q)$ is the calculated total energy of the supercell containing one V_O in charge state *q*, and $E_{tot}(In_2O_3)$ is the total energy calculated using the same supercell without a vacancy. The removed O atom is placed in an O reservoir of energy μ_O, which is referenced to the energy of an O atom in an isolated O_2 molecule. Note that, the chemical potential μ_O in Eq. (1) is not independent of the In chemical potential, because it has to satisfy the stability condition of In_2O_3,

$$2\mu_{In} + 3\mu_O = \Delta H_f(In_2O_3), \quad (2)$$

where μ_{In} is the chemical potential of In, which is referenced to the energy of an In atom in bulk In metal, and $\Delta H_f(In_2O_3)$ is the formation enthalpy of In_2O_3. In the growth or annealing processes, these chemical potentials can be varied by changing the In/O ratio, e.g., In-rich, O-rich, or anything in between. For the In-rich (O-poor) limit, $\mu_{In} = 0$ and $\mu_O = \Delta H_f(In_2O_3)/3$. For the O-rich (In-poor) limit, $\mu_{In} = \Delta H_f(In_2O_3)/2$ and $\mu_O = 0$. Because defects can exchange electrons with the host, the formation energy has to include the term qE_F, where E_F is the Fermi level, which is referenced to the valence band maximum (VBM) of the host crystal. An alignment of the electrostatic potential in a bulk-like region in the defect supercell with the potential of the perfect crystal is included. An expression analogous to Eq. (1) can be written for V_{In}.

The well-known band gap underestimation in semiconductors and insulators by DFT–LDA calculations makes the determination of the defect transition levels difficult and can also affect the values of formation energies. For In_2O_3, the binding energies of the bands related to the semicore In-*d* states are also underestimated by DFT–LDA. This causes the In-*d* states to appear too high and their interactions with the O *p* bands, which constitute the top of the valence band, becomes too strong. This effect also contributes to the band gap error in In_2O_3: the calculated fundamental band gap of In_2O_3 in LDA is only 1.17 eV, compared to the experimental value of 2.7 eV [17]. In order to overcome this problem, we applied an on-site Coulomb interaction to the semicore In-*d* states (LDA + *U* method), which partially corrects the band gap. By performing calculations for defect using both the LDA and LDA + *U*, we are able to acquire information on the change of transition levels and formation energies with respect to the band gap. After that, we can extrapolate the transition levels and formation energies to the experimental value of the band gap. The details of this approach can be found in Refs. [11,18]. In this work, a value of $U = 4$ eV for the In-*d* states is used. We estimated this value by calculating the *U* for the In atom ($U^{at} = 14.4$) and dividing it by the optical dielectric constant of In_2O_3 ($\varepsilon^{\infty} = 4$ [19]). The calculated lattice parameters, band gaps, and formation enthalpies of In_2O_3 using LDA and LDA + *U* are listed in Table 1, along with the experimental values.

Table 1
Calculated lattice parameters *a*, band gap E_g, and enthalpy of formation ΔH_f of In_2O_3 using LDA and LDA + *U*. The experimental values from Refs. [17,27,28] are also listed.

	LDA	LDA + *U*	Expt.
a (Å)	10.07	9.92	10.12
E_g (eV)	1.17	1.67	2.7
ΔH_f (eV)	−9.86	−10.41	−9.63

3. Results and discussions

The bixbyite structure of In_2O_3 contains 80 atoms in a conventional cell and 40 atoms in the primitive unit cell. It has two inequivalent In sites: In-8*b* (1/4, 1/4, 1/4) labeled In1, and In-24*d* (*u*, 0, 1/4) labeled In2; and one inequivalent O site: O-48*e* (*x*,*y*,*z*) in the Wyckoff notation. Both In1 and In2 are six-fold coordinated, surrounded by O atoms, while all O atoms are four-fold coordinated surrounded by In atoms. The conventional cell of In_2O_3 in the bixbyite structure and the calculated local structures are shown in Fig. 1. The local structure of In1 is highly symmetric; all six In–O bonds have the same length (slightly smaller than the averaged value of all In–O bonds). The local structure of In2 is less symmetric where there are three pairs of equivalent In–O bonds. The local structure of O is a distorted tetrahedron with all four In–O bonds inequivalent, with calculated bond lengths of 2.12, 2.17, 2.18 and 2.21 Å according to the LDA.

In the case of an oxygen vacancy (V_O) in the neutral charge state, an O atom is missing from an otherwise perfect crystal, leaving two electrons in a defect state which is a symmetric combination of four In dangling bonds. In the 2+ charge state, this state is unoccupied. In order to analyze the stability of the possible charge states of V_O in In_2O_3, we first inspect the band structure of the supercell containing V_O and compare it with that of the perfect bulk as calculated in the LDA. The band structures of a perfect In_2O_3 crystal and a neutral V_O in the same supercell are shown in Fig. 2(a) and (b), respectively. From examining Fig. 2(a) and (b), we can see that V_O significantly modifies the band structure of the supercell, resulting in new states that are a mixture of CB and defect states. Fig. 3 shows real-space charge density plots of the lowest conduction band states at Γ [Fig. 3(a) and (b), comparing bulk and a supercell containing V_O, respectively] as well as the next higher-energy state (~2.6 eV) at Γ and the state at 2.1 eV at *R* [Fig. 3(c) and (d)]. We can see that these states contain both CBM and defect character.

In the neutral charge state (V_O^0), three of the four In nearest neighbors relax outward by 4% (of the average equilibrium In–O bond length) while one In nearest neighbor slightly relax inward by about 3%. In the 1+ charge state (V_O^+), the state is singly occupied and all the four In nearest neighbors relax outward by about 7%.

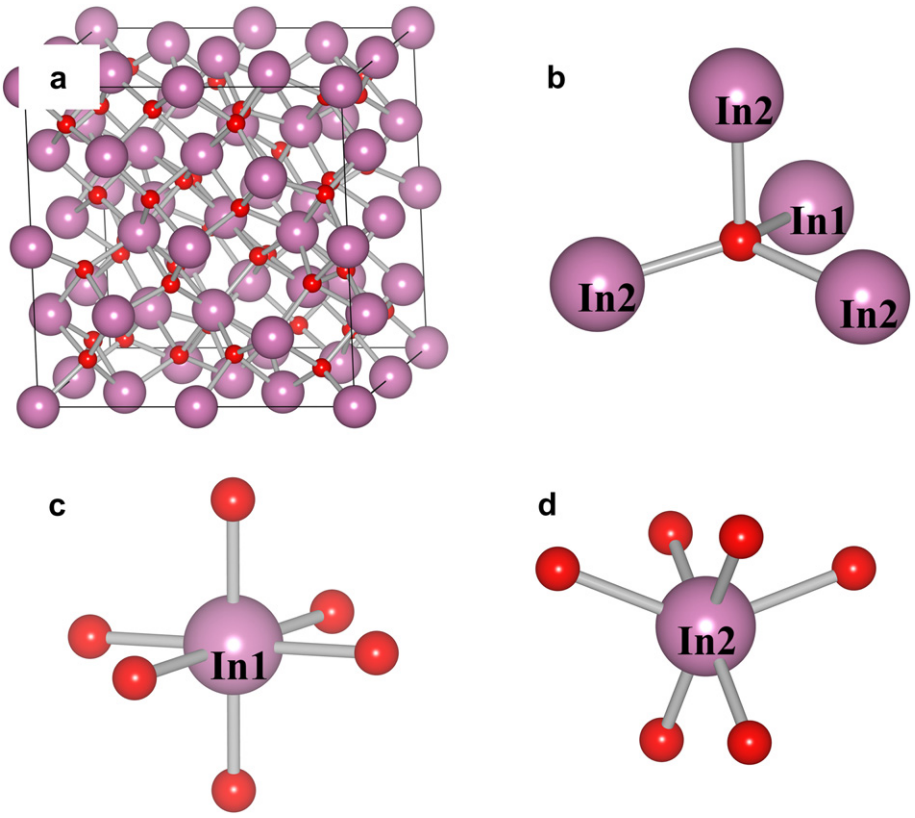

Fig. 1. (a) Conventional cell of the In_2O_3 bixbyite structure and local lattice structure of (b) O atom, and (c)–(d) In atoms at the 8*b* site and 24*d* sites, labeled by In1 and In2 respectively. Each of the In atoms is surrounded by six O whereas each O atom is surrounded by three In2 and an In1 atoms.

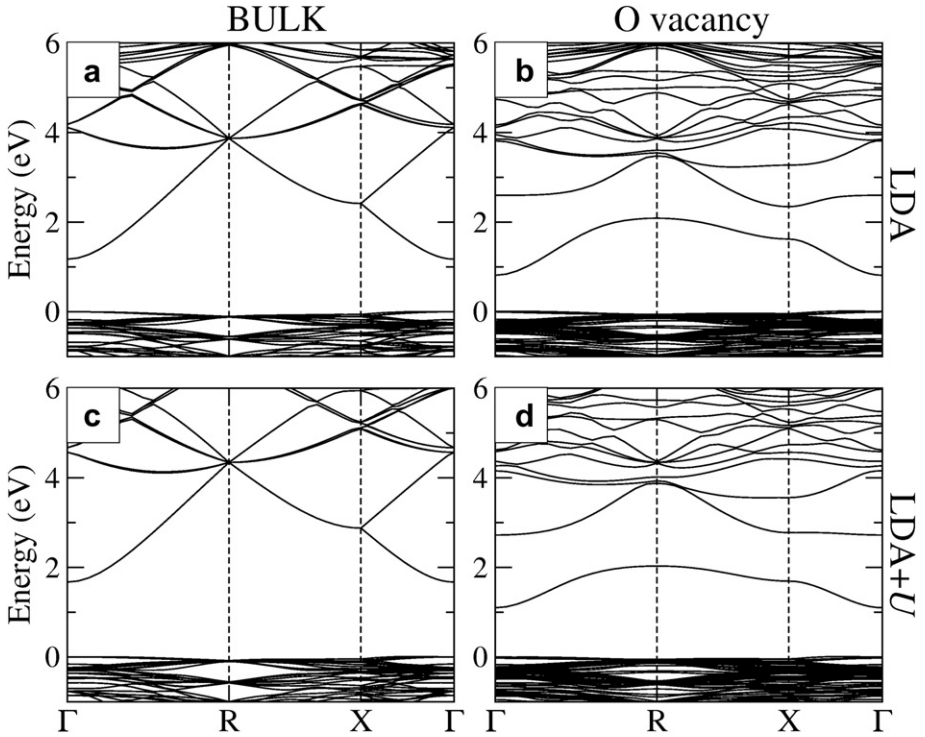

Fig. 2. Calculated band structures of the defect-free In_2O_3 80-atom supercell and of the same supercell containing an oxygen vacancy. (a) and (c) are for bulk, with (a) showing LDA and (c) LDA + *U* results. (b) and (d) are for V_O, with (b) showing LDA and (d) LDA + *U*.

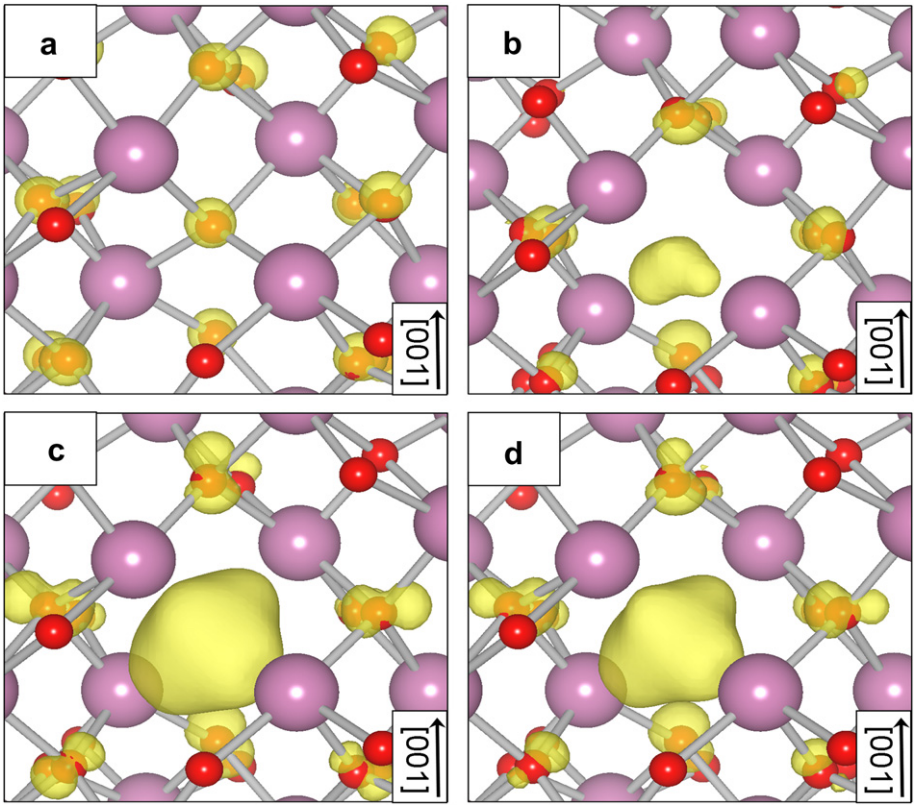

Fig. 3. Real-space charge density plot corresponding to (a) the CBM at Γ of defect-free bulk In_2O_3, (b) the Γ state at 0.8 eV of the supercell containing V_O, (c) the next higher Γ state at 2.6 eV, and (d) the lowest R state at 2.1 eV.

Finally, in the 2+ charge state (V_O^{2+}), the state is unoccupied and all the four In nearest neighbors relax outward by about 9% as shown in Fig. 4(a). These relaxations of V_O are similar to the case of V_O in ZnO [11], except that in neutral charge state all four Zn nearest neighbors are relaxed inward.

Because the band gap in the LDA is much smaller than the experimental value, it is difficult to draw firm conclusions about the properties of V_O in In_2O_3 based solely on an LDA calculation. E.g., it is unclear if the defect (V_O) state would be raised along with the CB when a band gap correction is applied. Therefore we repeat the same procedure of plotting the band structures using the LDA + U [Fig. 2(c) and (d)]. The band gap increases by 0.50 eV, i.e., from 1.17 eV in the LDA to 1.67 eV in the LDA + U, and the V_O-related states are shifted up as well. However, an inspection of Kohn–Sham states is insufficient to derive conclusions about the shallow or deep nature of the donor. This can only be decided based on transition levels obtained from formation energies for different charge states, as discussed below.

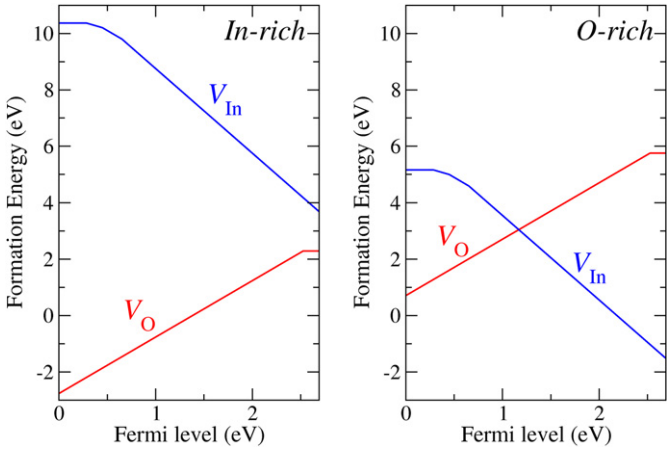

Fig. 4. Calculated formation energies as a function of Fermi level for the oxygen vacancy and indium vacancy in In_2O_3. Results for both In-rich and O-rich are shown. The Fermi level varies from 0 to 2.7 eV corresponding to the experimental band gap of In_2O_3.

For the In vacancy, an indium atom is missing from the crystal. This leaves six O dangling bonds and three holes for the neutral charge state (the missing In atom would contribute three electrons). These O dangling bonds hybridize into partially occupied states (with p-state characteristics) just above the VBM. These states can accept up to three electrons, making V_{In} stable in the neutral, 1−, 2− and 3− charge states. Because the six O nearest neighbors are too far away from each other to form chemical bonds, they significantly relax outward (8–11%; depending on the charge state). V_{In}^0 has the smallest relaxations and V_{In}^{3-} has the largest relaxations. Because there are two inequivalent In species in In_2O_3 [see Fig. 1(c) and (d)], there are two possible types of indium vacancies; V_{In1} and V_{In2}. By symmetry, for V_{In1} all six O nearest neighbors uniformly relax outward. For V_{In2}, four O neighbors relaxed outward by a large amount, while the other two O neighbors are only slightly relaxed outward.

Fig. 4 shows the formation energies of V_O and V_{In} as a function of Fermi level. The calculations using the LDA + U approach with the extrapolation [11] showed that V_O has a negative-U behavior, i.e., V_O^{2+} is a stable charge state (at almost the entire Fermi energy), V_O^+ is energetically unstable, and V_O^0 is stable in a limited range. The transition level $\varepsilon(2+/0)$ is found to be at 0.2 eV below the CBM

based on LDA and LDA + U calculations with extrapolation to get the results for the experimental band gap. Regardless of how deep V_O is, if one tries to dope In_2O_3 p-type, V_O certainly will counteract the doping and be one of the causes that make p-type doping difficult.

For indium vacancies, the formation energy of V_{In1} is lower than that of V_{In2} but by only 0.1–0.2 eV. The difference is quite small and therefore we do not need to discuss these defects separately; in Fig. 4, we show only the formation energy of V_{In1}. The transition levels of V_{In1} are $\varepsilon(0/-) = 0.29$ eV, $\varepsilon(-/2-) = 0.45$ eV, and $\varepsilon(2-/3-) = 0.65$ eV referenced to the VBM (the corresponding values for V_{In2} are 0.23, 0.55 and 0.79 eV). Under p-type conditions, the formation energy of V_{In} is very high even under the most favorable O-rich conditions. Because of this high formation energy as well as the large ionization energy, V_{In} is unlikely to serve as a source for conducting holes. Indium vacancies can therefore not make In_2O_3 p-type, as was claimed in Ref. [20]. Under n-type conditions, i.e., when the Fermi energy is near the CBM, the formation energy of V_{In} is the lowest (for the 3− charge state). This means that V_{In} can act as a compensating acceptor under n-type conditions. However, under In-rich conditions, the formation energy of V_{In} is still very high such that it is unlikely to form. Our results show that V_{In} can degrade the electron conductivity needed for transparent conducting applications. However, it has a high formation energy under In-rich conditions and will form only under relatively O-rich conditions.

It would be desirable to have experimental confirmation of the computational results that have been presented here. Various experimental techniques are available that may provide information about point defects. Vacancy defects in semiconductors can be experimentally studied by positron annihilation spectroscopy (PAS), a technique which can probe the concentration and stability of both cation and anion vacancies. An example of such a study, in the case of ZnO, is given in Ref. [21]. X-ray photoelectron spectroscopy (XPS) is a powerful tool that has been used to study vacancies in other oxides [22]. XPS allows probing work functions, surface states, and electronic state in the band gap of TCO as well as other semiconductor thin films; such states may reflect the presence of point defects at surfaces [23–26]. Powerful light sources generated by synchrotron facilities are becoming increasingly important for the investigations of point defects in TCOs.

4. Conclusions

We have presented an investigation of the electronic and structural properties of vacancy defects in In_2O_3 based on density functional theory using LDA and LDA + U functional, along with an extrapolation procedure to correct the band gap. These calculations give the $\varepsilon(2+/0)$ transition of the oxygen vacancy at about 0.2 eV below the CBM. Therefore, it remains unclear whether V_O is a shallow or deep donor. Regardless of how deep or shallow V_O is, if one tries to dope In_2O_3 p-type, V_O could counteract the doping and likely to be one of the causes that make p-type doping difficult. V_{In} is found to act as triple acceptor with very high formation energy in p-type In_2O_3, and is unlikely to be a source of p-type conductivity. The low formation energy of V_{In}^{3-} in n-type In_2O_3 indicates that it can be a compensation center for n-type doping, leading to carrier reduction.

Acknowledgements

This work is supported by the Thailand Research Fund (Grant No. RTA5280009), NANOTEC (NN-B-22-DI2-20-51-09), the NSF MRSEC Program (DMR05-20415), and by the UCSB Solid State Lighting and Energy Center. P.R. and X.Z. acknowledge the Max Planck Society (MPG), the Korea Ministry of Education, Science and Technology (MEST), Gyeongsangbuk-Do and Pohang City for the support of the Independent Junior Research Group at the Asia Pacific Center for Theoretical Physics (APCTP). S.L. thanks C.H. Park for useful discussions.

References

[1] Y. Kanai, Jpn. J. Appl. Phys. 23 (1984) L12.
[2] I. Hamberg, C.G. Granqvist, K.F. Berggren, B.E. Sernelius, L. Engström, Phys. Rev. B 30 (1984) 3240.
[3] T. Koida, H. Fujiwara, M. Kondo, Jpn. J. Appl. Phys. 46 (2007) L685.
[4] S. Limpijumnong, P. Reunchan, A. Janotti, C.G. Van de Walle, Phys. Rev. B 80 (2009) 193202.
[5] R.L. Weiher, J. Appl. Phys. 33 (1962) 2834.
[6] H.K. Müller, Phys. Status Solidi B 27 (1968) 723.
[7] J.H.W. De Wit, J. Solid State Chem. 8 (1973) 142.
[8] J.I. Jeong, J.H. Moon, J.H. Hong, J.S. Kang, Y.P. Lee, Appl. Phys. Lett. 64 (1994) 1215.
[9] L.-j. Meng, M.P. dos Santos, Appl. Surf. Sci. 120 (1997) 243.
[10] J.H.W. De Wit, J. Solid State Chem. 20 (1977) 143.
[11] A. Janotti, C.G. Van de Walle, Phys. Rev. B 76 (2007) 165202.
[12] A.K. Singh, A. Janotti, M. Scheffler, C.G. Van de Walle, Phys. Rev. Lett. 101 (2008) 055502.
[13] G. Kresse, J. Furthmüller, Comput. Mater. Sci. 6 (1996) 15.
[14] G. Kresse, J. Furthmüller, Phys. Rev. B 54 (1996) 11169.
[15] P.E. Blöchl, Phys. Rev. B 50 (1994) 17953.
[16] G. Kresse, D. Joubert, Phys. Rev. B 59 (1999) 1758.
[17] A. Bourlange, D.J. Payne, R.G. Egdell, J.S. Foord, P.P. Edwards, M.O. Jones, A. Schertel, P.J. Dobson, J.L. Hutchison, Appl. Phys. Lett. 92 (2008) 092117.
[18] A. Janotti, D. Segev, C.G. Van de Walle, Phys. Rev. B 74 (2006) 045202.
[19] I. Hamberg, C.G. Granqvist, J. Appl. Phys. 60 (1986) R123.
[20] J. Stankiewicz, F. Villuendas, R. Alcala, Appl. Phys. Lett. 96 (2010) 192108.
[21] F. Tuomisto, V. Ranki, K. Saarinen, D.C. Look, Phys. Rev. Lett. 91 (2003) 205502.
[22] Q.-H. Wu, A. Thissen, W. Jaegermann, M. Liu, Appl. Surf. Sci. 236 (2004) 473.
[23] A. Klein, Mater. Res. Soc. Symp. Proc. 666 (2001) F1.10.1.
[24] A. Klein, Appl. Phys. Lett. 77 (2000) 2009.
[25] Y. Gassenbauer, A. Klein, Solid State Ionics 173 (2004) 141.
[26] P. Ebert, K. Urban, L. Aballe, C.H. Chen, K. Horn, G. Schwarz, J. Neugebauer, M. Scheffler, Phys. Rev. Lett. 84 (2000) 5816.
[27] R.W.G. Wickoff, Crystal structures, second ed. Wiley, New york, 1964.
[28] D.R. Lide, CRC handbook of chemistry and physics. CRC Press, Boca Raton, Florida, 2004.